

It is also interesting to compare this result with the clock paradox where the ages of two twins differ by an amount  $\delta t$  after a round trip lasting for a time  $t$ . The fractional change in age is simply the fractional amount by which the traveling clock slows down. Hence,

$$1 - \delta t/t = (1 - v^2/c^2)^{1/2}, \quad (7)$$

and for  $v \ll c$ ,

$$\delta t/t \approx v^2/2c^2. \quad (8)$$

It follows from Eqs. (6) and (8) that if an angular change  $\theta$  occurs during a trip at constant speed  $v$  (e.g., in turning around there would be a change of  $\pi$ ), there will be a change in the direction indi-

cated by a gyroscope given by

$$\alpha/\theta = \delta t/t = v^2/2c^2. \quad (9)$$

Both observers will agree on the time difference and on the change in spatial direction. In both cases the change is caused by accelerations into new inertial frames. Since there is a common cause, the clock paradox and the Thomas precession are often treated at the same time in advanced texts on relativity.

<sup>1</sup> L. H. Thomas, *Nature* **117**, 514 (1926); *Phil. Mag.* **3**, 1 (1927).

<sup>2</sup> W. H. Furry, *Amer. J. Phys.* **23**, 517 (1955).

<sup>3</sup> R. M. Eisberg, *Fundamentals of Modern Physics* (Wiley, New York, 1961, 1967), p. 340.

## Thomson's $e/m$ Experiment Revisited

MICHAEL GLASCOCK\*

D. M. SPARLIN

*University of Missouri—Rolla*

*Rolla, Missouri 65401*

(Received 17 January 1972; revised 11 April 1972)

*The objective of this experiment is to familiarize the student with the impulse theorem, electron dynamics, and magnetic field contours. He is challenged to obtain accurate as well as precise measurements with suboptimum apparatus through correct analysis. He also investigates the influence of various systematic errors using model calculations on a small computer.*

### INTRODUCTION

This paper reports the outcome of an attempt to determine  $e/m$  for electrons in the Thomson geometry using the Heath-Berkeley CRT apparatus. The results of the investigation demonstrate the existence of systematic error as the values of  $e/m$  asymptotically approach the standard value as the range of observation of the path in the deflecting field is increased.

The charge to mass ratio of the electron was first measured by J. J. Thomson in 1897.<sup>1</sup> Subsequent methods of determining  $e/m$  are placed in historical perspective in the older text by Stranathan<sup>2</sup> and more recently in the text *The Taylor Manual*.<sup>3</sup> The most recent publication of the use of commercial cathode ray tubes in the Thompson form of the  $e/m$  experiment was that by Weber and McGee in 1939.<sup>4</sup>

Thomson performed his experiment with an evacuated cathode ray tube similar to that shown in Fig. 1. The crossed electric and magnetic fields were assumed to be uniform within the space designated by the circle. The magnitudes of the

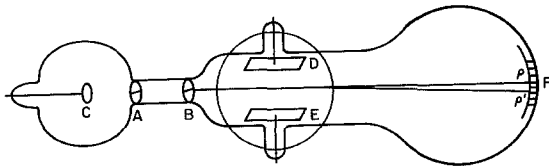


FIG. 1. Schematic diagram of J. J. Thomson's  $e/m$  apparatus. Discharge from electrode C to A generated a beam defined by the slits in A and B. A uniform electric field between D and E was balanced by the Lorentz force arising from the magnetic field confined to the same space as the electric one. This experiment was characterized by small angle deflections and the crossed field velocity determination.

electric and magnetic forces on the electron beam within this deflection region were considered to be equal and opposite. This feature was essential to the determination of the electron velocity. His analysis for  $e/m$  assumed small angle deflections of the beam under the action of the magnetic field alone and was quite straightforward as a consequence. The analysis presented in this paper does not assume either uniformity of the magnetic field or small angle deflections of the beam. Simplicity is therefore lost, as the student is required to apply a technique of numerical double integration in determining the value of  $e/m$ .

The following section presents a general theory for  $e/m$  in the Thomson configuration of transverse magnetic deflection field. This is followed by a description of the apparatus and procedure and finally a discussion of the *a posteriori* attempts to locate the source of the obvious systematic error in the values obtained for  $e/m$ . All numerical calculations were performed in the BASIC language on a Hewlett Packard 2114B 8K memory mini-computer.

**THEORY**

Suppose an electron is accelerated through a potential difference  $V_0$  along the  $x$  direction. If there are no other fields present it will travel along a straight-line path at a constant speed  $U$ , given by

$$U = (2eV_0/m)^{1/2} \tag{1}$$

where  $m$  is the mass of the electron and  $e$  its charge.

A constant magnetic field applied in the  $+z$  direction results in a deflection of the electron path. This field is cylindrically symmetric about the  $z$  axis and decreases in intensity away from the coil axis. This solenoidal field is zero in the  $x-y$  plane at a radius shown by the dashed circle in Fig. 2. Since the Lorentz force operates at right angles to the motion of the electron, the electron's path of motion will be confined to the  $x-y$  plane. Furthermore, its speed,  $U$ , will remain constant and equal to that given by Eq. (1). A typical path is indicated by the solid curve in Fig. 2.

The Lorentz force is given by

$$F_y = eV_x B_z(x, y), \tag{2}$$

where  $V_x$  is the velocity of the electron in the  $+x$  direction, and  $B_z(x, y)$  is the magnetic field strength in the  $z$  direction as a function of coordinates  $(x, y)$  measured from the axis of the coil. Since  $B_z(x, y)$  is cylindrically symmetric, we abbreviate our notation to  $B_z(R)$ , where  $R$  is the distance from the coil axis to a particular point along the electron trajectory in the  $x-y$  plane.

From Fig. 2 and elementary calculus it is possible to see that the velocity components  $V_x$  and  $V_y$  are given by

$$V_x = U \cos\theta = dx/dt \tag{3}$$

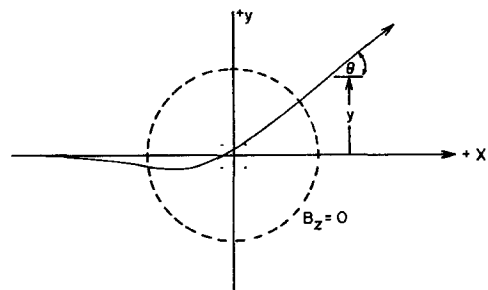


FIG. 2. Typical deflection curve for the path of the electron in the X-Y plane. As the electron nears the space between the Helmholtz coils its initial deflection is negative due to the fringing flux. As it enters the large field region, it passes through the  $B_z=0$  ring where the flux changes direction. The deflection plot shows an inflection point here. The major deflection occurs near the center of the coils with another inflection point observed as the electron leaves the field space.

and

$$V_y = U \sin\theta = dy/dt, \tag{4}$$

where  $\theta(t)$  is the angle between the electron's instantaneous velocity and the  $x$  axis. The angle  $\theta$  is defined by

$$\theta = \arctan(dy/dx), \tag{5}$$

where  $y$  is the displacement of the electron in the  $x$ - $y$  plane as a function of time, or position  $x$ . According to Newton's second law in *impulse form*, the relationship between  $V_y(t)$  and  $F_y(t)$  is given by

$$V_y(t) = m^{-1} \int_{t_0}^t F_y(t') dt' + V_y(t_0), \tag{6}$$

where  $V_y(t_0)$  is the  $y$ -axis velocity at  $t_0$ , the time of initial observance.

The integral of Eq. (4) provides an expression for the displacement  $y(t)$  in the form

$$y(t) = \int_{t_0}^t V_y(t) dt + y(t_0). \tag{7}$$

Substituting Eq. (6) into Eq. (7) leads to the complete expression for  $y(t)$ :

$$y(t) = m^{-1} \int_{t_0}^t \int_{t_0}^{t'} F_y(t'') dt'' dt' + \int_{t_0}^t V_y(t_0) dt + y(t_0). \tag{8}$$

We substitute for  $F_y(t)$  from Eq. (2) to give

$$y(t) = \frac{e}{m} \int_{t_0}^t \int_{t_0}^{t'} V_x(t'') B_z(R'') dt'' dt' + \int_{t_0}^t V_y(t_0) dt + y(t_0). \tag{9}$$

Since our measurement of the path of the electron is made with respect to coordinates  $(y, x)$  instead of  $(y, t)$ , we make a change of variables from  $t$  to  $x$  using the relation

$$dx/dt = U \cos\theta(x). \tag{10}$$

The result is

$$y(x) = \frac{e}{mU} \int_{x_0}^x [\cos\theta(x)]^{-1} \int_{x_0}^{x'} B_z(R'') dx'' dx + \int_{x_0}^x \frac{V_y(x_0) dx}{U \cos\theta(x)} + y(x_0). \tag{11}$$

Substituting of Eq. (4) for  $V_y$  at  $x_0$  and Eq. (1) for  $U$  into Eq. (11) leads to the expression

$$y(x) = \left(\frac{e}{2mV_0}\right)^{1/2} \int_{x_0}^x [\cos\theta(x)]^{-1} \int_{x_0}^{x'} B_z(R'') dx'' dx + \sin\theta(x_0) \int_{x_0}^x \frac{dx}{\cos\theta(x)} + y(x_0). \tag{12}$$

Solving for  $e/m$  gives the final expression

$$\frac{e}{m} = 2V_0 \left[ y(x) - y(x_0) - \sin\theta(x_0) \int_{x_0}^x \frac{dx}{\cos\theta(x)} / \int_{x_0}^x [\cos\theta(x)]^{-1} \int_{x_0}^{x'} B_z(R'') dx'' dx \right]^2. \tag{13}$$

Equation (13) simplifies to Thomson's equation

$$e/m = 2V_0 Y^2 (LB_z D)^{-2},$$

when  $B$  is uniform over diameter  $D$ ,  $\theta(x)$  is near zero,  $L$  is the distance to a fixed screen, and  $Y$  is the observed deflection at the fixed screen.

The constants of integration,  $y(x_0)$  and  $\sin\theta(x_0)$ , are determined by a least-square fit of a Taylor's expansion of  $y(x)$  to second order about  $x_0$ .

The basic assumptions upon which this analysis of  $e/m$  is based are: (1) that the deflection curve

$y(x)$  is known; (2) that the constants of integration  $y(x_0)$  and  $\sin\theta(x_0)$  are properly determined from a least-squares fit of a power series expansion of  $y(x)$  about  $x_0$ ; (3) that the magnetic induction  $B_z(R)$  is known and is cylindrically symmetric; and (4) that the electron speed is constant.

### EXPERIMENTAL APPARATUS AND PROCEDURE

The apparatus used in our version of this experiment is shown in Fig. 3. The cathode-ray tube supplied with the Berkeley Physics Lab-

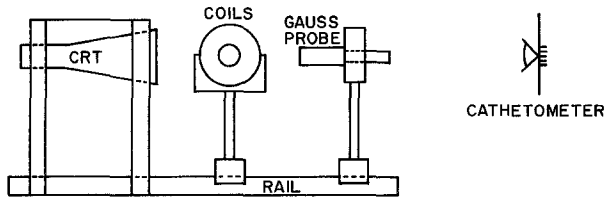


FIG. 3. The configuration of the experiment showing the CRT mounted over the aluminum rail. The deflection coils are moved with respect to the CRT to vary the point along the path of the electron at which it strikes the phosphor screen. The Hall probe is moved along a diameter of the deflection coils during the field calibration, after which it is removed to allow a free sight line for the cathetometer.

oratory apparatus provided the source of electrons, the vacuum flight path, and the screen which indicated the deflection  $y(x)$ . The CRT and socket base were inverted and four wooden legs were attached to suspend it over a rail. The rail provides definition of the  $x$  axis and supports the deflection coils and Hall probe.

The two deflection coils were held rigid and parallel on a holder made of copper tubing with a wooden base. The coils provided with the Berkeley apparatus could have been used, but the substitutes were more convenient due to their smaller weight. The coils are operated at constant current and centered at the height of the zero coil current spot on the CRT screen.

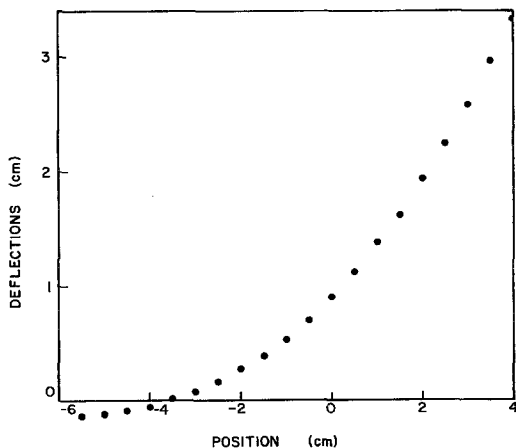


FIG. 4. A plot of the deflections of the CRT spot as a function of the screen to center of coil distance. The data shown are entirely with the  $B_z=0$  radius and do not demonstrate the inflection point.

A F. H. Bell Model 120 gaussmeter with Hall probe active element and zero field accessory were used in measuring  $B_z(R)$ . The active element was mounted on a sliding holder and could be moved from the center of the coil toward large  $x$ . The field was determined along a radius only, after the cylindrical symmetry was certified. A two-hour warm up was necessary to reduce drift on the low scales.

The  $y$  deflection was measured using a cathetometer placed at the end of the rail. A telescopic sight allowed operation well outside the range of the magnetic field. The  $y$  deflection sensitivity was determined to be 0.1 mm.

The rail was nonmagnetic and was built from aluminum and wood with brass screws. A meter

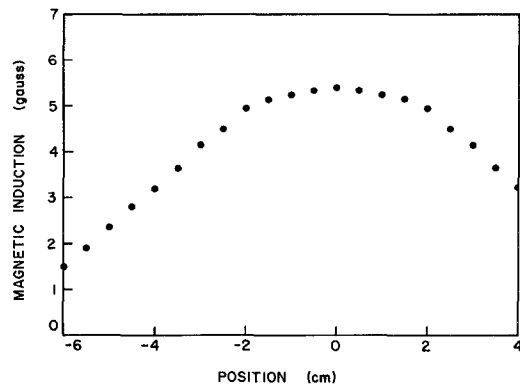


FIG. 5. A plot of the magnetic field strength as a function of the distance from the center of the coils.

stick was attached to the rail to facilitate measurement of the distance  $x$  between the Hall probe and the center of the coils, and between the center of the coils and the CRT screen when the  $y(x)$  are being determined.

The path followed by the electron is determined by observing the deflection of the spot on the CRT screen as a function of the distance from the screen to the center of the deflecting coils. The electron beam is assumed to enter the magnetic field region with  $V_y=0$  for all  $x$ . This assumption allows us to consider that the coil is fixed in space and that the phosphor screen is moved to intercept the beam at various points along its path. The finite length of the CRT used may violate this assumption and contribute to the observed systematic errors.

**ANALYSIS AND CONCLUSIONS**

The constants  $y(x_0)$  and  $\sin\theta(x_0)$  were determined from a Taylor's expansion of  $y(x)$  using the first few deflection readings near  $x_0$ . The accelerating potential,  $V_0$ , the magnetic induction,  $B_z(R)$ , and the deflection,  $y(x)$  were used in Eq. (13) to calculate a value of  $e/m$  for each position  $x$ . [A plot of the deflection  $y(x)$  is shown in Fig. 4. A plot of the magnetic induction  $B_z(R)$  is shown in Fig. 5.]

A plot of the value of  $e/m$  calculated at each position  $x$  is shown in Fig. 6. Notice that the values of  $e/m$  indicate the presence of systematic error

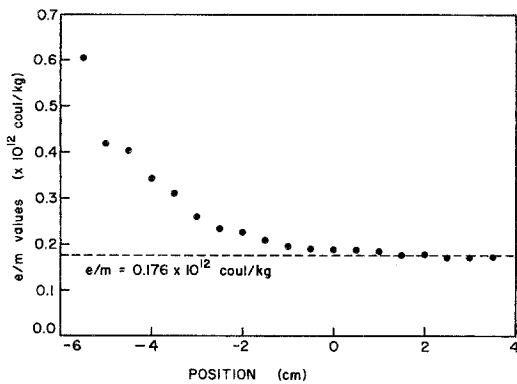


FIG. 6. A plot of the values of  $e/m$  calculated for each end point of the integration,  $X$ . The first observation of the deflections  $Y(X)$  was taken at  $-6$  cm from the center of the coil ( $X_0 = -6$  cm). The calculated values for  $e/m$  asymptotically approach the accepted value as the range of integration is increased. This behavior is characteristic of the existence of systematic error.

by their asymptotic approach to a constant,  $0.17 \times 10^{12}$  C/kg. The random error is not large and indicates that the data is *precise* but lacks in *accuracy*. The correct value of  $e/m$  is  $0.176 \times 10^{12}$  C/kg and is indicated by the horizontal dashed line. Our results are asymptotic to a value less than the standard value by about 5%.

A search for the probable source of this systematic error was conducted. The availability of a small computer for student use makes it possible to easily vary the experimental constants in searching for blunders.

The first possible source of error to be investigated was a constant term omitted from the

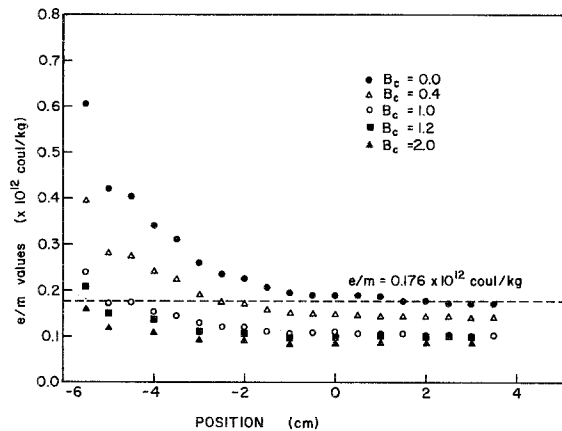


FIG. 7. A demonstration of the effects of adding arbitrary constants to the observed magnetic field strengths on the values of  $e/m$ . The addition of 1 G to each and every reading results in a flattening of the results, although at much too small a value.

magnetic induction. This may occur due to inaccurate zeroing or subsequent drift of the Hall probe. The effect of the addition of various arbitrary constants to the field values is shown in Fig. 7. The addition of a constant tends to flatten the curve, but depresses the average value far below the standard value of  $e/m$ .

The second source of error investigated was the scale factor for  $B$  which might arise from incorrect calibration of the gaussmeter. Results of this study

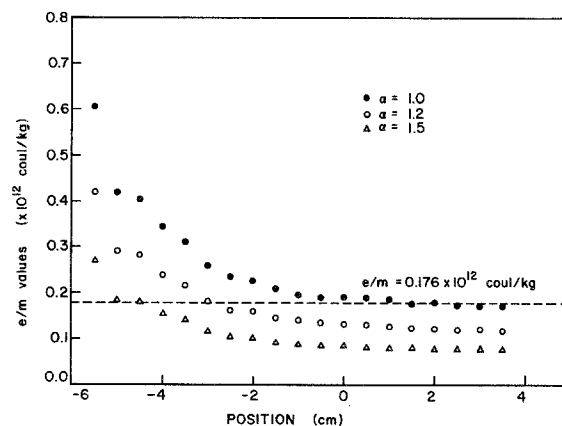


FIG. 8. A demonstration of the effect of scaling the measured magnetic field by the factor  $\alpha$ , such as would be necessary if the incorrect scale had been read. The result is to scale the systematic behavior without reducing its percentage effect.

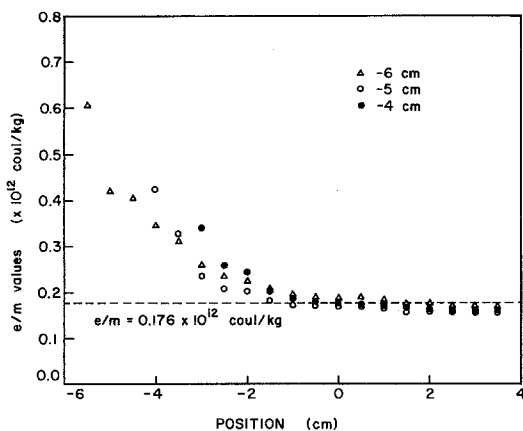


FIG. 9. This plot shows the effect of beginning the integration at  $-6$ ,  $-5$ , and  $-4$  cm from the center of the coil. Since the resulting curves fall along the same general asymptotic curve we are confident that the mathematical procedure is correct and that the systematic error is inherent in the raw data.

are shown in Fig. 8. In this case, the curves tend to be parallel to each other without substantially reducing their curvature, the prime indicator of systematic error. The calibration of the gaussmeter is not a likely source of the systematic error.

The third possibility for error was thought to be the starting position of the calculations,  $x_0$ . Perhaps the relative distance of the electron gun

from the coils was a factor. Figure 9 shows the results of starting the calculations at different position,  $x_0$ , along the deflection curve. These results show that the calculations are being properly done. The likely source of our error would seem to be a combination of zero offset in both the  $y$  and  $x$  coordinates and incorrect calibration factor for the magnetic field measurements.

Although this experiment fails to result in the accepted value for  $e/m$  free of systematic error, its other merits tend to uphold its practical value as a realistic and relevant advanced undergraduate physics lab experiment. The combination of the impulse theorem, electron dynamics, and magnetic field contour plotting provides a worthwhile exercise for the student. (This experiment is one of several assigned as "jobs" in a "role-playing" modern physics laboratory for juniors.<sup>5</sup>) In this version of the classic  $e/m$  experiment advanced students are assigned to determine to what extent intrinsic experimental difficulties can be overcome in a  $e/m$  experiment using the Heath apparatus in spite of its suboptimal design.

#### ACKNOWLEDGMENTS

Appreciation is expressed to Ed Blankenship, Dwight Carmichael, Arthur Loepp, and James Moore for their contributions to the development of this experiment.

\* Michael Glascock, BS Physics, Univ. of Missouri—Rolla, 1971, presently at Physics Dept., Iowa State, Ames, Iowa.

<sup>1</sup> J. J. Thomson, *Phil. Mag.* **44**, 293 (1897).

<sup>2</sup> J. D. Stranathan, *The "Particles" of Modern Physics* (Blakiston, New York, 1942).

<sup>3</sup> *The Taylor Manual* (Addison-Wesley, Reading, Mass., 1961), pp. 394–404.

<sup>4</sup> A. H. Weber and J. F. McGee, *Amer. J. Phys.* **7**, 62 (1939).

<sup>5</sup> A more complete report of our experience with this program is being prepared for publication. In short, each student member serves as research group leader at least once. The faculty advisor is President of UMR, Inc., as well as chief mechanic. Assignments range from maintenance and calibration services through testing apparatus and designing new experiments.